

## Shear behavior of DFRCC coupling beams using PVA and steel fiber

\*Toshiyuki Kanakubo<sup>1)</sup>, Yuriko Ozu<sup>2)</sup> and Keisuke Namiki<sup>3)</sup>

<sup>1)</sup> Dept. of Eng. Mechanics and Energy, Univ. of Tsukuba, Ibaraki, 305-8573, Japan

<sup>2)</sup> Technical Research Inst., Sumitomo Mitsui Const. Co., Ltd., Chiba, 270-0132, Japan

<sup>3)</sup> GSSIE, Univ. of Tsukuba, Ibaraki, 305-8573, Japan

<sup>1)</sup> [kanakubo@kz.tsukuba.ac.jp](mailto:kanakubo@kz.tsukuba.ac.jp)

### ABSTRACT

Ductile fiber-reinforced cementitious composite (DFRCC) is expected to provide sufficient shear performance of coupling beams in high-rise buildings under severe seismic loads and decrease the deterioration of energy absorption performance. This study focuses on shear behavior of coupling beams through anti-symmetrical loading test of beam specimens using PVA and steel fiber-reinforced cementitious composite. The test parameters are fiber types and the volume fraction of fiber. The shear capacity is evaluated by using tensile strength of DFRCC obtained by four-point bending test of test pieces. The shear capacities of DFRCC beams with higher volume fraction can be evaluated by adding the effect of fiber-carrying capacity to calculated shear capacity in the case of no-fiber.

### 1. INTRODUCTION

Ductile Fiber-Reinforced Cementitious Composite (DFRCC), which shows a deflection hardening branch and multiple cracking under bending stress, have been focused by lots of researchers because of its unique mechanical performance. In other hand, Engineered Cementitious Composite (ECC), which has been introduced by Li (Li 1993), exhibit a maximum tensile strain of several percent owing to the synergetic effect of high-performance fiber under pure tension. Unprecedented high-performance structural members by ECC have already been applied to seismic components such as coupling beams (Kanda et al. 2006).

The authors have studied the structural performance of beam-column joints in high-rise RC buildings using DFRCC in the panel zone (Sano et al. 2015, Yamada et al. 2016). These studies have reported that beam-column joints using DFRCC shows less damages and small crack opening compared with conventional concrete members.

---

<sup>1)</sup> Professor

<sup>2)</sup> Research Engineer

<sup>3)</sup> Graduate Student

DFRCC can also make it possible to improve durability and sustainable use of structures. However, it is difficult to evaluate tensile characteristic of DFRCC and structural performance of seismic components.

In the case of ECC, it is not so difficult to evaluate its tensile characteristic because of strain hardening behavior. Tensile stress increases after first cracking, and tensile stress carrying capacity does not start failing until cracks saturating. For example, bi-linear model with hardening branch or perfectly elastic-plastic model can be applied to express the tensile stress-tensile strain relationship for ECC (Rokugo and Kanda 2012). In fact, the authors have proposed the evaluation method of tensile strength of ECC by four-point bending test results as the material test of ECC (Kanakubo et al. 2007). In the case of DFRCC, however, its tensile stress generally starts decreasing after peak load in pure tension stress field. So, it is difficult to confirm the carrying tensile stress by DFRCC on its softening branch in seismic components.

The objective of this study is to confirm the structural performance of coupling beams as seismic components using DFRCC by various types of fibers and fiber volume fraction. The same methodology with tensile strength evaluation of ECC is carried out, i.e., four-point bending test as the material test of DFRCC is conducted. The specimens modeling coupling beams used in high-rise RC buildings are loaded by anti-symmetrical bending moment manner to simulate stress field in earthquake force.

## 2. OUTLINE OF LOADING TEST FOR BEAM SPECIMENS

### 2.1 Specimen

Fig. 1 shows the dimensions of beam specimen and Table 1 shows the specimens list. The total length of the specimen is 1,960mm. The central portion of 660mm length is the test region which is subjected to the anti-symmetrical bending moment. The depth ( $D$ ) and width ( $b$ ) of cross-section is 220mm and 160mm, respectively. Three steel deformed rebars D16 (SD490) were arranged as tension longitudinal reinforcements. Steel deformed rebars D4 (SD295) was arranged as stirrups at 120mm interval in the test region. Total of five specimens were tested.

The test parameters are types of fiber for DFRCC and volume fraction of fiber. PVA fiber with 0.10mm diameter and steel fiber with 0.16mm diameter were used. Fiber

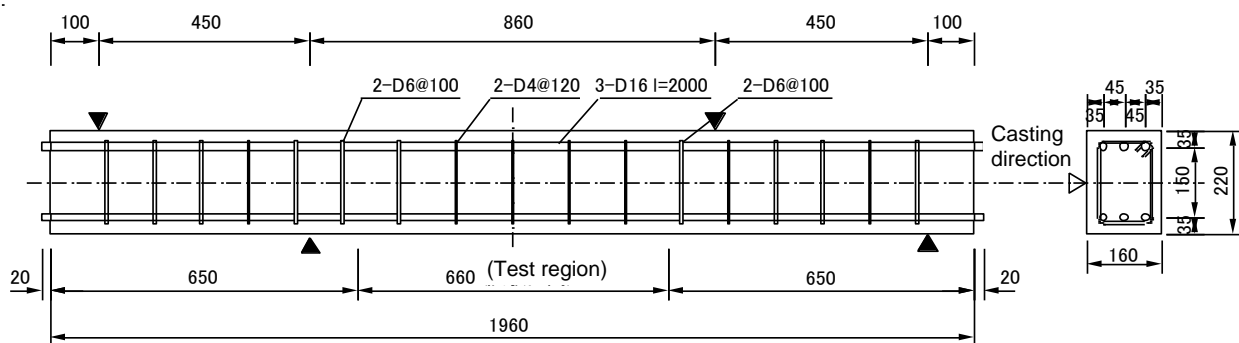


Fig. 1 Specimen dimensions

volume fraction was set to 1.0% and 2.0% for PVA fiber, 0.5% and 1.0% for steel fiber. Table 2 shows the dimensions and mechanical properties of fibers. To investigate the effect of fibers, mortar without fiber was used for specimen No.1. Table 3 lists the mechanical properties of steel rebars.

Table 1 Specimen list

ID	Common factor	Fiber type	Fiber volume fraction
No.1	Cross-section: 160x220mm	—	—
No.2	Shear span: 330mm ( $M/QD=1.5$ )	PVA	1.0%
No.3	Tension bar: 3-D16 (SD490)	PVA	2.0%
No.4	Stirrup: 2-D4@120 (SD295)	Steel	0.5%
No.5		Steel	1.0%

Table 2 Mechanical properties of fiber



Fiber type	Diameter (mm)	Length (mm)	Tensile strength (MPa)	Elastic modulus (GPa)	Appearance
PVA	0.10	12	1200	28	
Steel	0.16	13	2825	210	

Table 3 Mechanical properties of steel rebar

Type	Tensile strength (MPa)	Yield strength (MPa)	Elastic modulus (GPa)	Remarks
D16 (SD490)	714	513	196	Longitudinal bar
D4 (SD295)	548	391	180	Stirrup

## 2.2 Loading and measurement

The monotonic loading following anti-symmetric bending moment manner (Ohno-type shear test method) was carried out. The bending moment diagram is shown in Fig. 2. Applied shear force ( $Q$ ) can be obtained by 0.344 times applied force ( $P$ ).

To avoid shear failure outside the test region, both ends of beam specimen were jacketed by steel plates with 22mm thickness as shown in Fig. 3. Steel round bars were subjected through the steel plates at both loading points and supports.

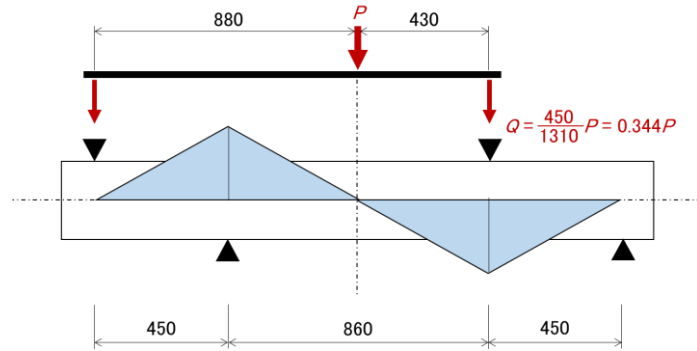


Fig. 2 Bending moment diagram

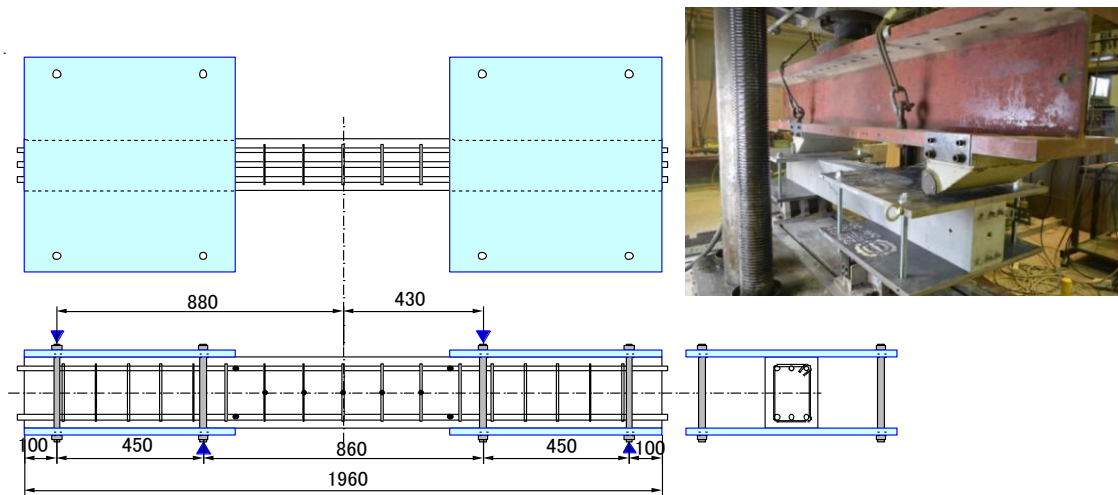


Fig. 3 Steel plate jackets for beam specimen

Two LVDTs were set to measure loading point displacements via holding jig fixing at the supporting points of the beam specimen as shown in Fig. 4. Assuming the rotation of rigid bodies of the specimen ends jacketed by the steel plates, translational angle ( $R$ ) is obtained from relative displacement at the center of the specimen ( $\delta$ ) divided by clear span length.

The strains of stirrups and longitudinal bars at the both ends of clear span were measured by strain gauges.

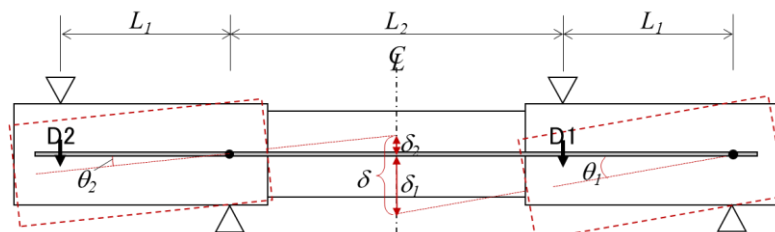


Fig. 4 Steel plate jackets for beam specimen

### 3. TENSILE CHARACTERISTICS OF DFRCC BY FOUR-POINT BENDING TEST

#### 3.1 Specimen and loading method

Table 4 shows the mixture proportion of DFRCC and compression test results by  $\phi 100\text{mm} \times 200\text{mm}$  cylinder test pieces at the age of loading of beam specimens. Used cement was high-early-strength Portland cement, fly ash was Type II of Japanese Industrial Standard (JIS A 6202), and sand was size under 0.2 mm. The high-range water-reducing admixture and thickening agent were added.

The specimen dimensions for four-point bending test are 100mm x 100mm in cross-section, and 400mm in length, these follows JCI-S-003-2007 “Method of test for bending moment–curvature curve of fiber-reinforced cementitious composites” (JCI 2007). Axial deformations at upper and lower side in constant moment region were measured by pi-type LVDTs as shown in Fig. 5. Three specimens were tested for one-type of DFRCC.

Table 4 Mixture proportion of DFRCC

Type	Unit weight ( $\text{kg/m}^3$ )					Comp. strength (MPa)	Elastic modulus (GPa)
	Water	Cement	Sand	Fly ash	Fiber		
PVA 1.0%	380	678	484	291	13	45.3	16.8
PVA 2.0%					26	43.1	15.7
Steel 0.5%					39	44.5	16.6
Steel 1.0%					78	42.2	17.2

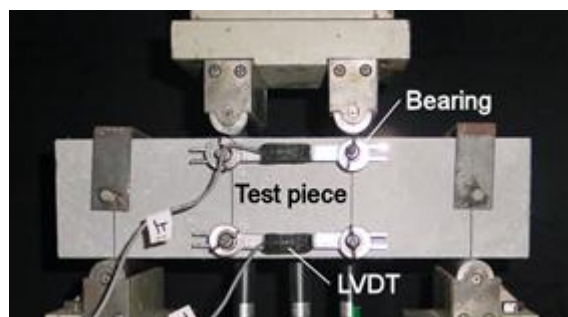


Fig. 5 Four-point bending test for DFRCC

#### 3.2 Test results

Table 5 lists test results of four-point bending test of DFRCC. Some of specimens finally failed by the opening of crack which took place outside of LVDT. Curvature at maximum load could not be obtained in these specimens. All specimens showed deflection hardening behavior as that the load increased after first cracking.

Tensile strength and ultimate strain are calculated following Appendix of JCI-S-003-2007 “Evaluation method for tensile strength and ultimate tensile strain of fiber-

reinforced cementitious composites” (JCI 2007). In this evaluation method, tensile strength can be calculated under the assumption that the tensile stress distributes as a constant manner in tension zone of the section. Though this assumption is mostly accepted in the case of ECC, it is considered that the actual stress distribution in the case without strain hardening DFRCC is different from the assumed distribution.

The curvature at maximum load could not be measured by LVDT for specimens of steel 1.0%, these values are assumed to have same one with the average of specimens of steel 0.5%. As the calculation results, averages of tensile strength of the specimen of PVA 1.0% and PVA 2.0% are 1.25MPa and 1.90MPa, respectively. Those of steel 0.5% and steel 1.0% are 2.08MPa and 1.76MPa.

Table 5 Test results of four-point bending test of DFRCC

Type	At maximum load		Calculation result		
	Bending moment (kN·m)	Curvature (1/m)	Tensile strength (MPa)	Ultimate strain (%)	Average of tensile strength (MPa)
PVA 1.0%	0.562	0.172	1.18	1.58	1.25
	0.528	0.093	1.16	0.82	
	0.424	0.004	1.41	0.02	
PVA 2.0%	0.869	0.162	1.88	1.44	1.90
	0.866	0.088	1.93	0.74	
	0.737	—*1	—	—	
Steel 0.5%	0.945	0.056	2.21	0.45	2.08
	0.872	0.067	1.95	0.56	
	0.686	—*1	—	—	
Steel 1.0%	0.891	—*1	1.76	(0.61)*2	1.76
	0.923	—*1	1.83		
	0.839	—*1	1.69		

\*1: Specimen failed by crack out of LVDTs.

\*2: Curvature at maximum load is assumed to be same with steel 0.5% specimen.

## 4. TEST RESULTS OF BEAM SPECIMENS AND DISCUSSIONS

### 4.1 Failure progress

Beam specimens after loading are shown in Fig. 6. Cracks are traced by a pen after loading. At first, small bending cracks took place at the ends of clear span in tension zone. After that, diagonal shear cracks were observed in the central part of the specimens. In specimen No.1, the shear crack widely opened at the same time of yielding of stirrups, and cover mortar fell from the specimen. In other specimens, small shear cracks took place in sequence, and maximum load was observed at the same time of localizing of crack opening. Falling of covers were not observed in specimens



from No.2 to No.5. In all specimens, yielding of stirrups was observed at the maximum load.

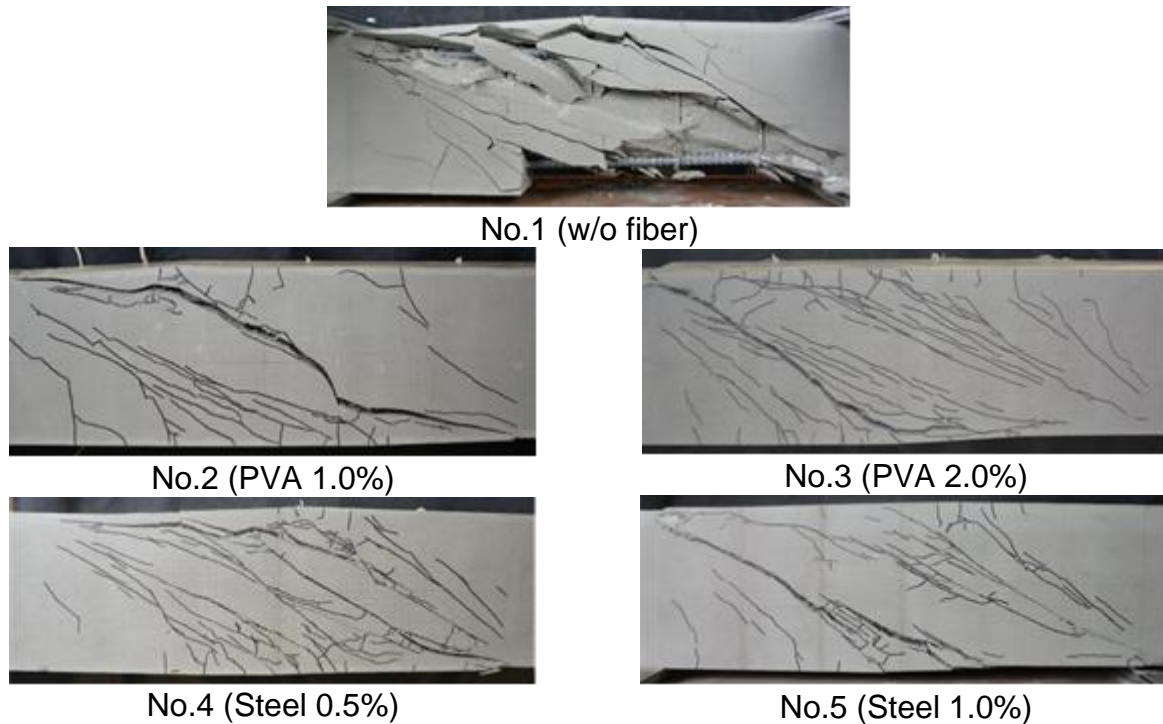


Fig. 6 Specimens after loading

#### 4.2 Shear force-translational angle curve

Fig. 7 shows shear force ( $Q$ )-translational angle ( $R$ ) curves of all specimens. Except for specimen No.2 (PVA 1.0%), the maximum shear force of the specimens with fibers are larger than that of specimen No.1 (w/o fiber). It is considered that shear force is carried also by fiber bridging.

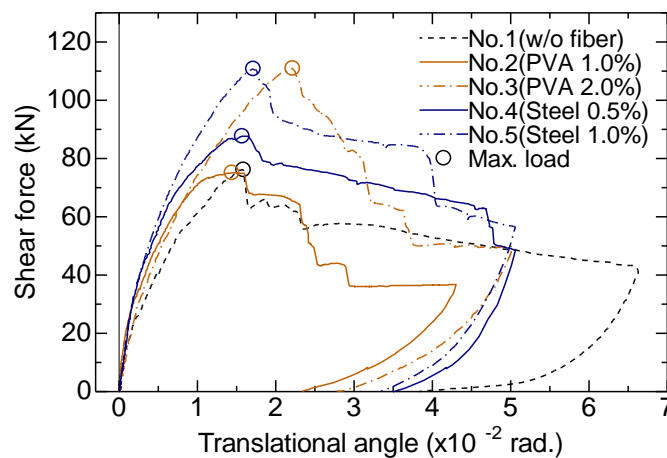


Fig. 7 Shear force-translational angle curve

Comparing the curves of specimens No.1 and No.2, though the maximum shear force is almost same, shear force until maximum load in specimen No.2 is larger than specimen No.1. It is assumed that the effect of fiber bridging in specimen No.2 vanished before reaching maximum load. Comparing the curves of specimens No.4 (Steel 0.5%) and No.5 (Steel 1.0%), the curves show almost similar tendency until  $R=0.6 \times 10^{-2}$  rad. After that, an increment of shear force in specimen No.4 becomes smaller than specimen No.5. It is also assumed that the effect of fiber bridging in specimen No.4 starts decreasing before reaching maximum load. The reducing of shear force after maximum load are larger in PVA specimens (No.2 and No.3).

#### 4.3 Shear capacity of beam specimens

In the case of ECC, the evaluation method of shear capacity of beam has been propose by Eq.(1) (Kanakubo et al. 2007). This formula consists of shear capacity by truss and arch mechanism, and fiber bridging. The former two items are same as the case of the conventional RC beams. Shear capacity by fiber bridging is simply added to consider the contribution of tensile stress of DFRCC. In this study, the same evaluation method is adopted for evaluation of shear capacity of DFRCC beams.

$$V_{su} = V_t + V_a + V_f \quad (1)$$

$$V_t = b \cdot j_t \cdot p_w \cdot \sigma_{wy} \cdot \cot \varphi \quad (2)$$

$$V_a = \tan \theta \cdot (1 - \beta) \cdot \nu \cdot \sigma_B \cdot b \cdot D / 2 \quad (3)$$

$$\tan \theta = \sqrt{(L/D)^2 + 1} \quad (L/D) \quad (4)$$

$$\beta = (1 + c \sigma^2 t \varphi) p_w \cdot \sigma_w / \nu \cdot c \quad (5)$$

$$\nu = 1.70 \sigma_B^{-0.333} \quad (6)$$

$$\cot \varphi = \min \left\{ \frac{2 \cdot \theta \cdot j_t}{D \cdot \tan \theta}, \sqrt{\frac{\nu \cdot \sigma_B}{p_w \cdot \sigma_{wy}}} \right\} \quad (7)$$

$$V_f = b \cdot j_t \cdot \nu_t \cdot \sigma_t \cdot \cot \varphi \quad (8)$$

where,

$V_{su}$  : shear capacity

$V_t$  : shear capacity by truss mechanism

$V_a$  : shear capacity by arch mechanism

$V_f$  : shear capacity by fiber bridging

$b$  : width of member

$j_t$  : distance between compression and tension bars

$p_w$  : stirrup ratio

$\sigma_{wy}$  : yield strength of stirrup

$\sigma_B$  : compressive strength of DFRCC

$\varphi$  : angle of compressive strut



- $\theta$  : angle of arch mechanism  
 $\nu$  : effective coefficient of compressive strength of DFRCC  
 $D$  : depth of member  
 $L$  : clear span length  
 $\nu_t$  : reduction factor for tensile strength of DFRCC  
 $\sigma_t$  : tensile strength of DFRCC

Table 6 lists the test results of shear capacity and calculation results by Eq.(1). The tensile strength of DFRCC listed in Table 5 is utilized for the calculation. Fig. 8 shows the comparison between the test results of shear capacity and calculation results. Both shear capacity is standardized by calculated flexural capacity of beam specimen considering fiber bridging in tension zone as indicated by Eq.(9) (Shimizu et al. 2007).

$$V_{fu} = \left\{ 0.9 \cdot a_t \cdot \sigma_y \cdot d + \frac{b \cdot D^2}{2} \sigma_t \right\} / (L / 2) \quad (9)$$

where,

- $V_{fu}$  : flexural capacity  
 $a_t$  : cross-sectional area of tension bars  
 $\sigma_y$  : yield strength of tension bars  
 $d$  : effective depth of member

As seen in Table 6 and Fig. 8, the calculated shear capacity overestimates the test results in the case of lower volume fraction of fiber, both in PVA and Steel. For the specimens with higher volume fraction, the ratio of test results to calculations is 0.95 and 0.98. It is considered that the shear capacities of DFRCC beams with higher volume fraction can be evaluated by adding the effect of fiber-carrying capacity to calculated shear capacity in the case of no-fiber. It is assumed that the effect of fiber bridging in specimens with lower volume fraction starts decreasing before reaching the shear capacity of beam.

Table 6 Shear capacity of beam specimen

Specimen	Test result (kN)	Calculation (kN)	Test / Calc.
No.1 (w/o fiber)	76.1	83.1	0.92
No.2 (PVA 1.0%)	75.1	105.9	0.71
No.3 (PVA 2.0%)	110.9	116.8	0.95
No.4 (Steel 0.5%)	87.7	121.6	0.72
No.5 (Steel 1.0%)	110.8	113.1	0.98

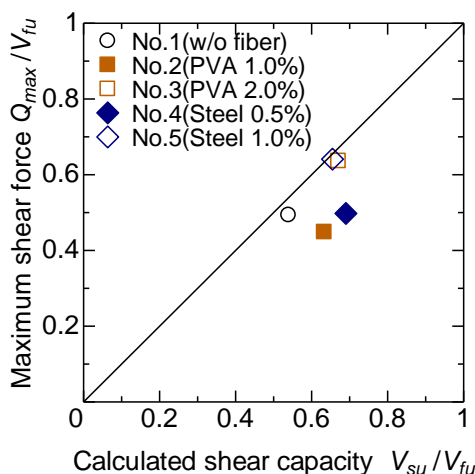


Fig. 8 Comparison of shear capacity

## 5. CONCLUSIONS

In this study, to evaluate shear behavior of seismic components using DFRCC with PVA and steel fibers, five beam specimens were subjected to anti-symmetrical bending moment loading. The tensile strength of DFRCC is evaluated by the four-point bending test results. The shear capacities of DFRCC beams with higher volume fraction can be evaluated by adding the effect of fiber-carrying capacity to calculated shear capacity in the case of no-fiber. It is assumed that the effect of fiber bridging in the case of lower volume fraction starts decreasing before reaching the shear capacity of beam.

## 6. REFERENCES

- JCI (Japan Concrete Institute). (2007), "Method of test for bending moment–curvature curve of fiber-reinforced cementitious composites", JCI-S-003-2007, [http://jci-net.or.jp/j/jci/study/jci\\_standard/JCI-S-003-2007-e.pdf](http://jci-net.or.jp/j/jci/study/jci_standard/JCI-S-003-2007-e.pdf).
- Kanakubo, T., Shimizu, K., Kanda, T., Nagai, S. (2007), "Evaluation of Bending and Shear Capacities of HPRFRC Members toward the Structural Application", *Proceedings of the Hokkaido University COE Workshop on High Performance Fiber Reinforced Composites for Sustainable Infrastructure System*, pp.35-44.
- Kanda, T., Tomoe, S., Nagai, S., Maruta, M., Kanakubo, T., Shimizu, K. (2006), "Full Scale Processing Investigation for ECC Pre-cast Structural Element", *Journal of Asian Architecture and Building Engineering*, Vol.5, No.2, pp.333-340.
- Li, V.C. (1993), "From Micromechanics to Structural Engineering -the Design of Cementitious Composites for Civil Engineering Applications", *JSCE J. of Struc. mechanics and Earthquake Engineering*, 10(2), pp.37-48.
- Rokugo, K., Kanda, T., ed. (2012), "Strain Hardening Cement Composites: Structural Design and Performance", State-of-the-Art Report of the RILEM Technical Committee 208-HFC, RILEM State-of-the-Art Reports 6

- Sano, N., Yamada, H., Miyaguchi, M., Yasojima, A., Kanakubo, T. (2015), "Structural Performance of Beam-Column Joint using DFRCC", *11th Canadian Conference on Earthquake Engineering -Facing Seismic Risk-*, Paper ID 94163
- Shimizu, K., Kudo, S., Kanakubo, T. (2007), "Scale Effect in Flexural and Shear Behavior on Ductile Reinforced Cementitious Composites", *Proceedings of the Japan Concrete Institute*, Vol. 29, No.3, 1429-1434. (in Japanese)
- Yamada, H., Ando, M., Yasojima, A., Kanakubo, T. (2016), "Effect of Fiber Types on Shear Performance of Precast Concrete Beam-Column Joints Using DFRCC", *The 7th International Conference of Asian Concrete Federation*, 3. Concrete structures, Paper No.46.